이학석사 학위논문

STAT1/2-mediated high order chromatin structure enhances therapeutic efficacy through viral mimicry in hepatocellular carcinoma

STAT1/2를 매개로 한 크로마틴 삼차구조가 간암의 세포독성 항암제 감수성에 미치는 역할 규명

2019년 2월

서울대학교 융합과학기술대학원

분자의학 및 바이오제약학과

남 지 원

Abstract

STAT1/2-mediated high order chromatin structure enhances therapeutic efficacy through viral mimicry in hepatocellular carcinoma

Ji Won Nam

Department of Molecular Medicine

and Biopharmaceutical Sciences

World Class University Graduate School

of Convergence Science and Technology

Seoul National University

Anti-tumor effects of chemotherapeutic agents are known to induce type I interferon signaling pathways that enhance the immunogenicity of dying cancer cells, and thereby stimulate anti-tumor immune response. The chemotherapeutic agent induced immune response is termed as viral mimicry, as these type I interferon related gene signatures are similar to those induced by viral pathogens. Here we demonstrate that treatment of chemotherapeutic agents stimulates rapid production of multiple interferon-stimulated genes (ISGs) via double-stranded RNAs derived from endogenous retroviruses in human hepatocellular carcinoma cells. Clustered ISG locus forms higher-order chromatin structure mediated by signal transducer and activator of transcription 1/2 (STAT1/2) during coordinate transcriptional regulation of these genes after chemotherapy. The finely tuned regulation of multiple ISGs transcription is abrogated when physical proximity is destroyed by STAT1 depletion. In addition, chemotherapeutic efficacy is abrogated when STAT1 expression is destroyed. Overall, our results suggest that transcriptional regulation of ISGs by STAT1/2-mediated higher-order chromatin structure is crucial for the efficient anti-tumor treatment

Keywords : STAT1/2; Higher-order chromatin structure; Type I interferon signaling; Endogenous retroviruses; Chemotherapeutic efficacy; Transcription

Student number : 2017-22991

Table of Contents

List of Tables

List of Figures

Introduction

Cancer immunosurveillance indicates that the immune system recognizes and eliminate premalignant cells to protect the host from tumor development [1, 2]. However, some of the cells eventually reduce their immunogenicity or develop capacity to establish immunosuppressive microenvironment and escape immune recognition [3, 4]. Although considerable amount of work has revealed the importance of immune system to constrain tumor growth [2], the molecular mechanism underlying how malignant cells regulate their immunogenicity to anti-tumor immunosurveillance remains an open question.

Until recently, the ultimate goal of conventional chemotherapy to kill malignant cells has been mainly focused on their ability to inhibit cell division, DNA replication, cellular metabolism and microtubule assembly [5]. However, recent preclinical and clinical data have illustrated that some of the chemotherapeutic agents does not only activate cytostatic/cytotoxic effects, but also immunogenic cancer cell death [2, 6]. Recent studies have demonstrated that cancer cell death after treatment of several chemotherapeutics, such as doxorubicin, oxaliplatin, and bortezomib, can release diverse danger signals to its neighboring cells through damage associated molecular patterns (DAMPs) [6-9]. These DAMPs are recognized by Pathogen Recognition Receptors (PRRs) of other cells to activate innate and adaptive immune system or to affect the tumor cell itself by modulating cell proliferation and expression of tumor associated antigens [10, 11].

Type I interferons (IFNs) are well known cytokines produced by multiple cell types to evoke immune response after viral and bacterial infection [11]. However, recent studies have shown that ionizing radiation (IR) or chemotherapy can also activate type I

IFN signaling pathway [6, 9]. Upon receiving type I IFN signals, signal transducer and activator of transcription 1 (STAT1) is activated by IFN receptor bound Janus kinase [11]. Phosphorylated STAT1 can enter the nucleus to regulate the induction of defined set of genes [11]. Since the transcriptional regulation should be tightly regulated in order to promote anti-tumor immune response as well as to limit excess toxicity [2, 8, 11], it is of great interest to understand how transcription factor STAT1 determine the fine-tune transcription of diverse type I IFN gene signatures.

Genomes are dynamically organized into a compact three-dimensional structure in nuclear space in a highly specific manner to facilitate diverse nuclear processes, such as DNA replication, DNA repair, and transcription [12-14]. Proper higher-order chromatin folding through binding of specific transcription factors are important for establishing functional interactions between cell/signal type specific promoters and enhancers [15, 16]. Physical proximity between co-regulated genes will bring high local concentrations of specific transcription factors and its transcriptional components, allowing cells greater control while reducing pressure for extremely sophisticated control [17, 18]. So, given the growing appreciation of chromatin structure as an important element regulating gene expression [19], we hypothesize that STAT1 mediates higher-order chromatin structure to facilitate transcriptional regulation of interferon-stimulated genes (ISGs) by physical proximity.

Here we demonstrate that treatment of chemotherapeutic agents induce viral mimicry through type I IFN-STAT1 signaling pathway after the recognition of double-stranded RNAs (dsRNAs) derived from endogenous retroviruses (ERVs) in human hepatocellular carcinoma (HCC) cells. The finely tuned transcriptional regulation of ISGs

are coordinately regulated by STAT1/2-mediated higher-order chromatin structure. Overall, our results demonstrate that transcriptional regulation of viral mimicry through STAT1/2-mediated higher-order chromatin structure is crucial for the efficient anti-tumor treatment in HCC cells.

Material and Methods

Reagents and cell culture

Oxaliplatin and 5-fluoruracil (5-FU) were obtained from Selleck Chemicals and administrated at conditions indicated in the figure legends. Polyinosinic:polycytidylic acid (poly (I:C)) was from Sigma-Aldrich. Human HCC cells (Hep3B, Huh7, SNU886, and SNU368) were purchased from the Korean Cell Line Bank. Cells were cultured in RPMI1640 from Hyclone Laboratories, supplemented with 10% heat inactivated fetal bovine serum and gentamicin (10 μg/ml) at 37 °C in a humidified 5% CO_2 atmosphere.

Reverse transcription and western blot analysis

2μg of total RNA was reverse transcribed as previously described [20]. Whole-cell extracts were prepared, and western blot analysis was performed as previously described [21].

Table 1-1. Primer sequences for RT-PCR and Quantitative real-time PCR

GENE	SEQUENCE (5' → 3')	
STAT1	F	CCGTTTTCATGACCTCCTGT
	R	TGAATATTCCCCGACTGAGC
STAT2	F	CCCAAACCTTCAGAACCAGC
	R	TGTCCAGCCATGTCCAGAAT
IFIT1	F	TCTCAGAGGAGCCTGGCTAA
	R	TCAGGCATTTCATCGTCATC
IFIT2	F	TGGTGGCAGAAGAGGAAGAT
	R	TGCACATTGTGGCTTTGAAT
IFIT3	F	CTGGGTGGAAACCTCTTCAG
	R	ATGGCATTTCAGCTGTGGA
IFIT5	F	CCTTCGCACCAAACTGACAA
	R	ATGGAAAGTCGGAGCTCACA
APOL2	F	CAGAGGAGGTTGAGCAGGTC
	R	GTGCCCGCAATTTGTTTACT
APOL6	F	CACCTGAAGGAAGGAGCAAG
	R	TCGCAGGTCCCAGTTAAATC
OAS1	F	TTGACTGGCGGCTATAAACC
	R	GAGCTCCAGGGCATACTGAG
OAS3	F	GTCAAACCCAAGCCACAAGT
	R	TGTAGGCACACCTGGTGGTA
IRF1	F	AGCTCAGCTGTGCGAGTGTA
	R	TAGCTGCTGTGGTCATCAGG
IRF3	F	GAGGTGACAGCCTTCTACCG
	R	TGCCTCACGTAGCTCATCAC
IRF9	F	CTGTCTGGAAGACTCGCCTG
	R	GTGCAGTTCTGCATGGCATC

Table 1-2. Primer sequences for RT-PCR and Quantitative real-time PCR

TLR3	F	AGCCTTCAACGACTGATGCT
	R	TTTCCAGAGCCGTGCTAAGT
RIG1	F	AGAGCACTTGTGGACGCTTT
	R	TGCAATGTCAATGCCTTCAT
MDA5	F	ACCAAATACAGGAGCCATGC
	R	GCGATTTCCTTCTTTTGCAG
ERVMER 34-1	F	TCCAGGAACGATGATGATGA
	R	AGAAGGCCTTTGGTTTGGTT
ERVFRD	F	AGCAGCCGTAGTCCTTCAAA
	R	AGGGGAAGAACCCAAGAGAA
ERVK 13-1	F	GTGTGGCTGTACCCCAGAGT
	R	ACACACCTTGCATTGGAACA
ERV 3-1	F	GGGAGTATGCGGAAAGTTCA
	R	CTCCAAGGGATGAGAACCAA
ERVV 1	F	TTAGCAGAGCAGGGTGGAGT
	R	AATGGACCCTGCTGAATCAC
ERVWE 1	F	CTAAATGGGGACATGGAACG
	R	CCAGTGTTTCGAAGCTCCTC

Growth inhibition assays

The viability of cells was assessed using MTT assays (Sigma-Aldrich) as described in our previous study [22]. A total of 3×10^3 cells were seeded in 96-well plates, incubated for 24 h, and treated for 72 h with indicated drugs at 37 °C. Following treatment, MTT solution was added to each well and incubated for 4 h at 37 °C. The medium was then removed, and dimethyl sulfoxide was added and mixed thoroughly for 30 min at room temperature. Cell viability was determined by measuring absorbance at 540 nm using a VersaMax microplate reader (Molecular Devices). The concentration of drug required to inhibit cell growth by 50% was determined via interpolation from dose-response curves using Calcusyn software (Biosoft, Ferguson). Six replicate wells were utilized for each analysis, and at least three independent experiments were conducted.

Viral transduction

For gene knockdown, two distinct single guide RNAs (sgRNAs) targeting each genes or control GFP were cloned into LentiCRISPRv2 vector (Addgene, #52961) [23] and transduced by virus using Virapower packaging mix (Invitrogen) in HEK293FT cells as described previously [21]. Transduced cells were selected in 1 μg/ml puromycin (Sigma-Aldrich) for 7 days. To make single clones, transduced cells were plated into 96-well plates by limiting dilution, and further expanded approximately 30 days. Silencing was validated by western analysis. The oligo sequences used for the sgRNA cloning are noted in Table 1.

RNA transfection

Total RNA was isolated using TRI reagent (Molecular Research Center) after treatment of 5 μM oxaliplatin or vehicles for 72 h in Hep3B cells. After then, 5 μg of RNAs were treated with 2 U/μg of RNase III (Ambion), 10 U/μg of RNase H (Invitrogen) or not for 30 min at 37 °C [6, 24, 25]. Subsequent to RNase treatment, RNA concentration was measured with a Nanodrop, and 2 μg of RNA was transfected into Hep3B recipient cells.

Chromatin immunoprecipitation (ChIP) assay and quantitative real-time PCR (qPCR)

ChIP assays were determined as previously described [21]. qPCR using SYBR Green (Molecular Probes) was conducted to observe enriched DNA using StepOnePlus (Applied Biosystems). The enrichment of target DNA over the input was calculated using the ΔΔCt method, and the results were presented as the mean ± SEM [21]. The PCR primers used for the ChIP and qPCR assays are listed in Table 2.

Table 2-1. Primer sequences for ChIP-PCR

GENE	SEQUENCE (5' → 3')	
IFIT - 1	F	CCGAACAGCTGAGAATTGCA
	R	TAGGAAGCTTGCCAGTGTGA
IFIT - 2	F	TTGCAGGTCTCAAGCCGTTA
	R	TCTGCTGTTCCGAAAAGCTG
IFIT - 3	F	GTGGTGCACGTCTGTAATCC
	R	GCCCTGAAAACTGACTCACG
IFIT - 4	F	CATTGGGTTTCTGCAGCACT
	R	CCAATGGTGTAAGCTGTGGG
IFIT - 5	F	AAGACTGGAGTGGAAGCAGG
	R	GAGTACGCTGAGTTCGCATG
OAS1	F	TCTTCTGGGATGGTGGTTTC
	R	TCACTGCAGAAATGGTGAGC
OAS3	F	GCACGTTTCTGAAATGCTCA
	R	CTTGGACCTGACACCCACTT
OAS2	F	TGTGTGTCCCTGAGCAAGTC
	R	CATCTGTAAGCTGGGGGA AA
ERVMER-pol2	F	GTCTGGCTTCCTAGGTCTGG
	R	GAGGAGAGGGTAATCGCGAA
ERVMER-max	F	GCACAGCCTCTATTGCCTTC
	R	GGCTCCAGGAATTCGTTGTC
ERVMER-CEBPB	F	AGATTGGAACCTGTGAGCCA
	R	GCCAAAACCAAACCAAAGGC
ERVFRD-pro	F	AGGAGCCACATGTGCATTTG
	R	AGCCAGTACCAGGGAAAGAC
ERVFRD-Ex1	F	GGCAATTGGAGCATGGAGAG
	R	TCCAACTACTGACTGCCCTG

Table 2-2. Primer sequences for ChIP-PCR

GENE	SEQUENCE (5' → 3')	
ERVFRD-Ex2	F	GAGCTGGCTATAGGTGAGGG
	R	GTCGATTCACCAATGCCTCC
ERVK-HNF4	F	TCCCAGTTCATCACCTGCTT
	R	CAACAGGTCTTGGCCCTCTA
ERVK-lni	F	AGATGGTCTCGCTCTTTCCG
	R	AATTGCCATTGACTCCAGCC
ERVK-Sin	F	GCAGCAAAAGCACCCAAATG
	R	TCTGTCTGTAGAGGAACCGC
ERV3-SETD2	F	AGTTCCAGGCAGCAGTTAGT
	R	TACCGCACCCCAGTTTACAT
ERV3-SETD	F	TGTTTGCCACTAGTCTCGGT
	R	GGCTCGCAAAGTTGGAAGAA
ERV3-5up	F	AGACTACACCAGAAGCTCCG
	R	GGAAGCTCTGCCTGAAAAGG
ERVV-1	F	CCAGGGTCACAAGTCCTCAT
	R	GGTTCTTCGGGACCTTCTCA
ERVV-2	F	ACTGTGAGAAGGTCCCGAAG
	R	AAGGAGAAGAACCGATGCCA
ERVV-4	F	AGGTAGCCAGACAAGAGCAG
	R	GAACAGAGGAATGCAGCCAC
ERVW-pro	F	TGGCACTTCACTCCATTTGC
	R	ATGACTAGGGTTGCTGGCAT
ERVW-body	F	TCCAGTGTTTCGAAGCTCCT
	R	CTCCCTAGCAGCAGTAGTCC
ERVW-3down	F	CTTCAGCTTGCAGGGGAATC
	R	ACACTCCCTTGCCTAACCTC

Chromosome conformation capture (3C) assay

A 3C assay was conducted as previously described [20] with minor modification. The cross-linked chromatin was digested with 1,000 U of EcoRI (NEB) at 37 °C overnight followed by ligation with 2,000 U of T4 DNA ligase (NEB) at 16 °C for 4 h with shaking at 800 rpm. To correct for different ligation efficiency between fragments and different PCR efficiency between primer sets, equimolar amounts of the BAC clone (RP11-1107P24 for IFIT locus) was digested with 200 U of EcoRI at 37°C overnight as previously described [20]. Relative cross-linking frequencies were determined by comparing DNA ligated between two fragments in 3C samples with DNA ligated randomly in control templates and then by normalizing to the ligation frequency in the HEMGN gene [20]. The PCR primers used for the 3C assay are noted in Table 3.

Table 3. Primer sequences for 3C-PCR

GENE	SEQUENCE (5’ → 3’)
IFIT – 2651	TCTGACTAAGCTGC TCCAGTG
IFIT – 18910	CCTCGAATAGAACATCTAGGAGACA
IFIT – 27795	TGTCTCAAAGTCCATCTTTGTGTT
IFIT – 38149	GGGAAGTGCAAGGAGTCAG
IFIT – 44842	GTTTCCCAGGACAACAGGAG
IFIT – 51230	GCCTTGCTCTCTGGTCAATC
IFIT – 73581	TTCTTGTCCCTTGGACTTGG
IFIT – 99019	CTTTCTATGGGGCACACGAC
IFIT – 138121	TGTCAAGCCCCTTCCTGATA
IFIT – 141761	TGATTTAATTCTCCATTCCTCCA
IFIT – 115732	CCTCTGTAAACAGATGGAGTTGG
OAS1 – 3C	TGCAGGGACAGTCACAGAAC
OAS3 – 3C	TGGGAGATCCAATGCTATGA

Deletion of STAT1/2 binding sites by CRISPR/Cas9 system

We constructed two sgRNAs which targeting the STAT1/2 binding region within IFIT1 gene such that the genomic sequences between two sgRNA-targeting sites could be deleted. A pair of two sgRNA were co-transduced into Hep3B cells by virus as described above. Then bulk cultures were plated clonally at limiting dilution. After approximately 30 days of clonal expansion, genomic DNA was extracted. Fragment deletions induced by sgRNAs were identified by PCR and direct sequencing.

Antibodies

Following antibodies were used in this study: STAT1 (9172S), STAT2 (4594S), p-STAT1 (7694S; Cell Signaling Technology); Actin (SC-1616), normal rabbit IgG (SC-2027) and RNA Pol II (SC-899; Santa Cruz Biotechnology); Acetylated histone H3 (06-599; Millipore) and H3K9me3 (ab8898; Abcam).

Results

Chemotherapy induces levels of ISGs with STAT1/2 activation in HCC cells

To identify whether transcriptional activation of ISGs after chemotherapy is associated with efficient cancer cell death, I treated increasing doses of oxaliplatin or 5-fluoruracil (5-FU) to four HCC cells showing different sensitivity to oxaliplatin or 5-FU. First, an accumulation and phosphorylation of H2AX was easily observed in Hep3B cells treated with increasing doses of oxaliplatin or 5-FU (Figure 1A). Next, I assessed sensitivity of Hep3B cells to oxaliplatin or 5-FU by colony forming assays. Oxaliplatin or 5-FU treatment markedly decreased both the number and the size of colonies formed by Hep3B cells (Figure 1B). I obtained similar results in other HCC cells (data not shown).

Next, to determine if chemotherapy can activate ISGs and its downstream effector genes, I performed quantitative RT-PCR (qRT-PCR) after oxaliplatin or 5-FU treatment in HCC cells. Hep3B showed significant transcriptional upregulation of ISGs (Figure 1C). Like Hep3B cells, Huh7 cells showed transcriptional upregulation of ISGs, whereas SNU368 or SNU886 cells showed little change (Figure 1G). Parallel with the activation of ISGs after oxaliplatin or 5-FU treatment, I found the phosphorylation of STAT1 and STAT2 at the tyrosine residue in Hep3B and Huh7 cells, hereafter referred to as an ISG-responder (Figure 1A and 1H). However, I could not detect the phosphorylation of STAT1 and STAT2 in SNU368 and SNU886, referred to as an ISG-non responder (Figure 1H).

To test whether STAT1 and STAT2 are a prerequisite for the expression of ISGs

after chemotherapy treatment, I disrupted the STAT1 and STAT2 expression using CRISPR/Cas9-Knockout (KO) system [26] in Hep3B and Huh7 cells, ISG-responder. I confirmed that the STAT1 and STAT2 protein levels were significantly decreased (Figure 1D) and the induction of ISGs were abrogated when oxaliplatin were treated in ISG-responder cells (Figure 1E and data not shown). Furthermore, I obtained that there was decreased sensitivity to oxaliplatin in STAT1/2-double KO clones of ISG-responder cells (Figure 1F and data not shown).

Taken together, these results suggest that chemotherapy can stimulate transcriptional induction of ISGs via activation of STAT1 and/or STAT2 in ISG-responder HCC cells.

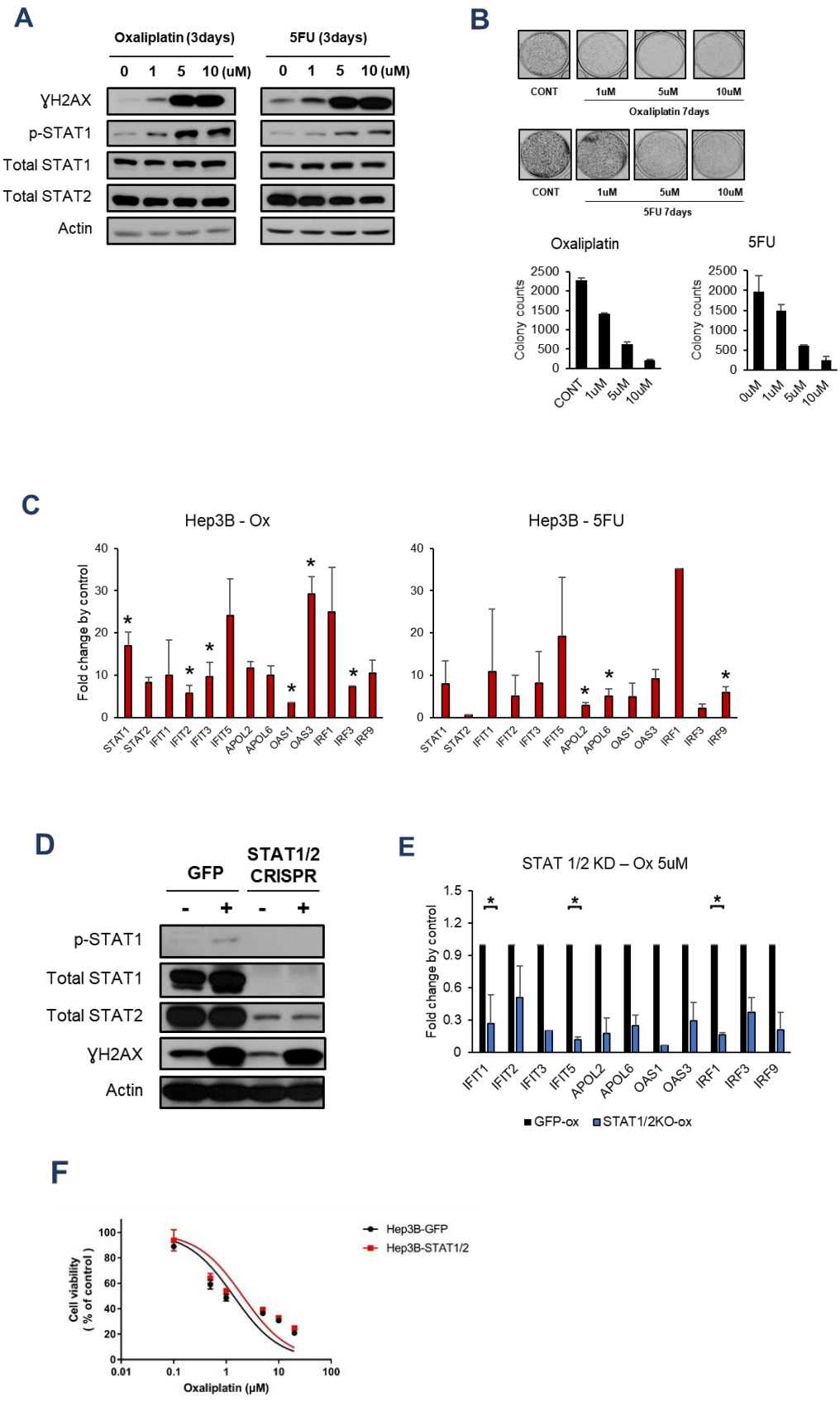
A
Oxaliplatin (3days)
5FU (3days)
0 1 5 10 (uM)
0 1 5 10 (uM)
γH2AX
p-STAT1
Total STAT1
Total STAT2
Actin
B
CONT
1uM
5uM
10uM
Oxaliplatin 7days
CONT
1uM
5uM
10uM
5FU 7days
Oxaliplatin
5FU
Colony counts
2500
2000
1500
1000
500
0
CONT
1uM
5uM
10uM
0uM
1uM
5uM
10uM
C
Hep3B - Ox
Hep3B - 5FU
Fold change by control
40
30
20
10
0
STAT1
STAT2
IFIT1
IFIT2
IFIT3
IFIT5
APOL2
APOL6
OAS1
OAS3
IRF1
IRF3
IRF9
D
GFP
STAT1/2 CRISPR
- + - +
p-STAT1
Total STAT1
Total STAT2
γH2AX
Actin
E
STAT 1/2 KD – Ox 5uM
Fold change by control
1.5
1.2
0.9
0.6
0.3
0
IFIT1
IFIT2
IFIT3
IFIT5
APOL2
APOL6
OAS1
OAS3
IRF1
IRF3
IRF9
GFP-ox
STAT1/2KO-ox
F
Cell viability (% of control)
100
80
60
40
20
0
0.01
0.1
1
10
100
Oxaliplatin (μM)
Hep3B-GFP
Hep3B-STAT1/2

Figure 1. Transcriptional activation of ISGs after Chemotherapy through STAT1/2 pathway

(A) Hep3B cells were treated with 0, 1, 5, or 10 μM of oxaliplatin or 5-FU for 3 days. Total cell extracts were prepared and western blot analysis was performed with indicated antibodies. Actin was used as loading control.

(B) The growth inhibitory effects of oxaliplatin or 5-FU were evaluated using a colony-forming assay after treatment of indicated amount of oxaliplatin or 5-FU for 7 days. The total surviving cells were counted. Error bars represent the SD, n = 3 biological replicates from independent experiment.

(C) Quantitative real-time PCR (qRT-PCR) analysis of ISGs expression in Hep3B after 5 μM of oxaliplatin or 10 μM 5-FU for 5 days. Relative levels of expression were normalized to 18S ribosomal RNA and untreated cells. Data are shown as mean ± SD (n=5). *$p < 0.05$.

(D, E) Hep3B cells were transduced with control (GFP) or STAT1/2-targeting lentiCRISPR vectors and selected in 1 μg/ml puromycin. After 7 days, transduced cells were plated into 96-well plates, and further expanded approximately 30 days to make single clone. Stable STAT1/2-double KO clone was treated with 5 μM oxaliplatin or vehicles for 3 days. (D) Western blots were performed with indicated antibodies. (E) mRNA expression of ISGs was analyzed by qRT-PCR. Relative levels of expression were normalized to 18S ribosomal RNA and untreated cells. Data are shown as mean ± SD (n=5). *$p < 0.05$.

(F) IC50 values for oxaliplatin were determined using the MTT viability assay. Untreated cells were considered 100% viable. *$p < 0.05$.

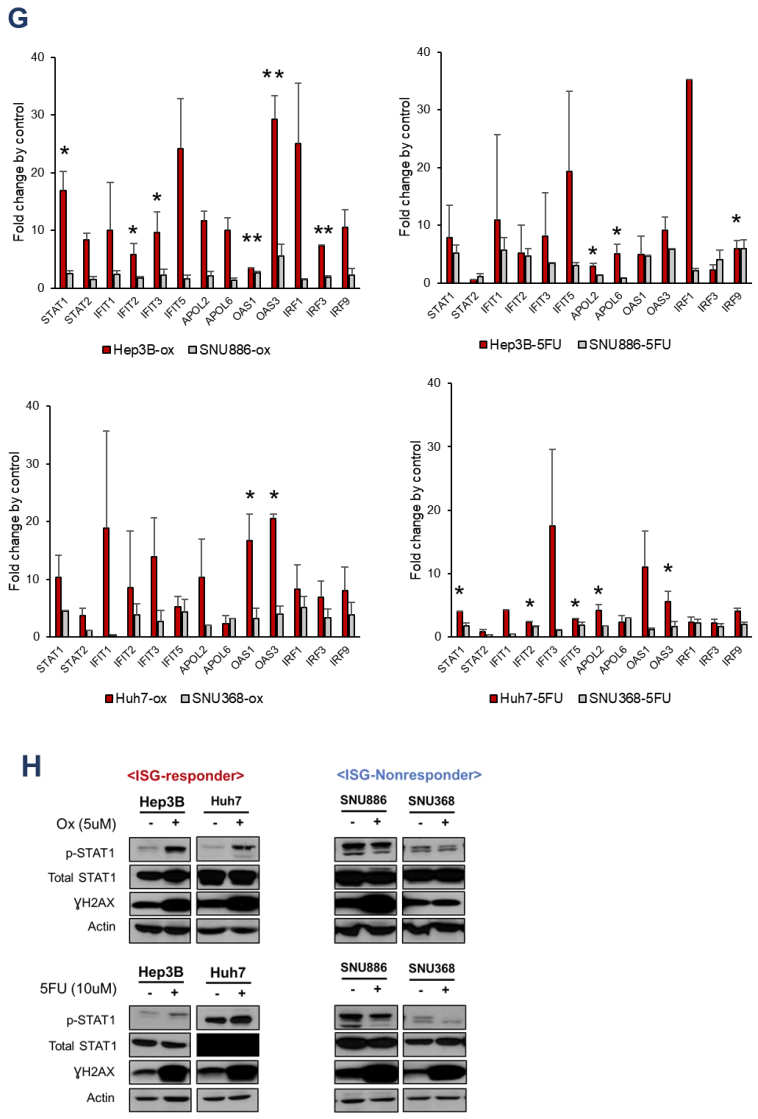

Figure 1.

(G-H) Hep3B, Huh7, SNU886, and SNU368 cells were treated with 5 μM of oxaliplatin or 10 μM of 5-FU for 3 days. (G) qRT-PCR analysis of ISGs expression in HCC cells after 5 μM of oxaliplatin or 10 μM 5-FU for 5 days. Relative levels of expression were normalized to 18S ribosomal RNA and untreated cells. Data are shown as mean ± SD (n=5). *$p < 0.05$. (H) Total cell extracts were prepared and western blot analysis was performed with indicated antibodies. Actin was used as loading control.

Cancer chemotherapy activates ISGs through viral mimicry

Although induction of type I IFN signaling pathway was identified on the basis of its ability to defend virus-derived nucleic acids [27], recent studies indicate that some of the endogenous RNAs, such as dsRNAs from ERVs, can also mimic viral infection during cancer treatment [25, 28]. In this regard, I hypothesized that viral mimicry after chemotherapy treatment in HCC cells was associated with dsRNA derived from ERVs. To confirm if chemoagents treatment triggers transcription of ERVs, I examined several ERVs with qRT-PCR. Interestingly, Hep3B and Huh7 cells, ISG-responders, showed significant upregulation of ERV transcripts after oxaliplatin or 5-FU treatment but not in ISG-non responders, SNU886 and SNU368 cells (Figure 2A and data not shown). ERVs are recognized by PRR such as Toll-like receptor 3 (TLR3), Retinoic Acid Inducible Gene 1 protein (RIG1) and Melanoma Differentiation-Associated protein 5 (MDA5) [10]. Interestingly, the treatment of oxaliplatin or 5-FU activated the expression of PRRs in Hep3B and Huh7 cells but not in SNU886 and SNU368 cells (Figure 2B). I also found that the disruption of TLR3 using CRISPR/Cas9-KO system [23] abrogates the chemoagent-mediated ISGs induction in Hep3B cells (Figure 2C), suggesting that PRR-mediated recognition of dsRNAs may be lead to the transcription of ISGs after chemotherapy.

To further validate whether or not dsRNA from ERVs are responsible for ISGs expression after chemotherapy, I extracted total RNA from oxaliplatin-treated and untreated Hep3B cells and incubated with Ribonuclease III (RNase III) or Ribonuclease H (RNase H) (Figure 2D) [24]. RNase III is an endoribonuclease that specifically digests

dsRNA to short dsRNA fragments, whereas RNase H only cleaves an RNA strand of RNA/DNA hybrids [25, 28]. After then, I transfected the same amount of RNase-treated total RNAs into Hep3B cells and subsequently measured the ISGs induction by qRT-PCR [6, 24, 25]. As expected, total RNAs from oxaliplatin-treated cells induced the ISG expression more than those from oxaliplatin-untreated cells (Figure 2D). However, the induction of ISGs by oxaliplatin-treatment was abrogated when the extracted RNA was degraded by RNase III (Figure 2D). RNase H also reduced the expression but the effect was moderate than RNase III (Figure 2D), Taken together, these results indicate that dsRNA derived from ERVs is crucial role for activation of ISGs by chemotherapy in Hep3B.

Although viral mimicry can be triggered by 5-aza-CdR, DNA methyltransferase inhibitors, [25, 28], however, I could not find any change of DNA methylation status near ERVs after chemotherapy in HCC cells (data not shown). Furthermore, 5-aza-CdR treatment had no effect on ERVs expression in HCC cells (data not shown), suggesting that the methylation status of ERVs do not appear to have a major role in the transcriptional activation of ERVs by chemotherapy in HCC cells. Next. to ask if chemotherapy changed the epigenetic landscape within the ERVs genes, I determined occupancy of histone H3 acetylation (AcH3), a mark of active transcription [29]. The enrichment of AcH3 increased significantly by oxaliplatin treatment (Figure 2E), whereas non-responder SNU886 cells showed no histone modification in response to oxaliplatin (data not shown). These results providing evidence that ERVs expression generated by chemotherapy is associated with epigenetic regulation of the ERV locus.

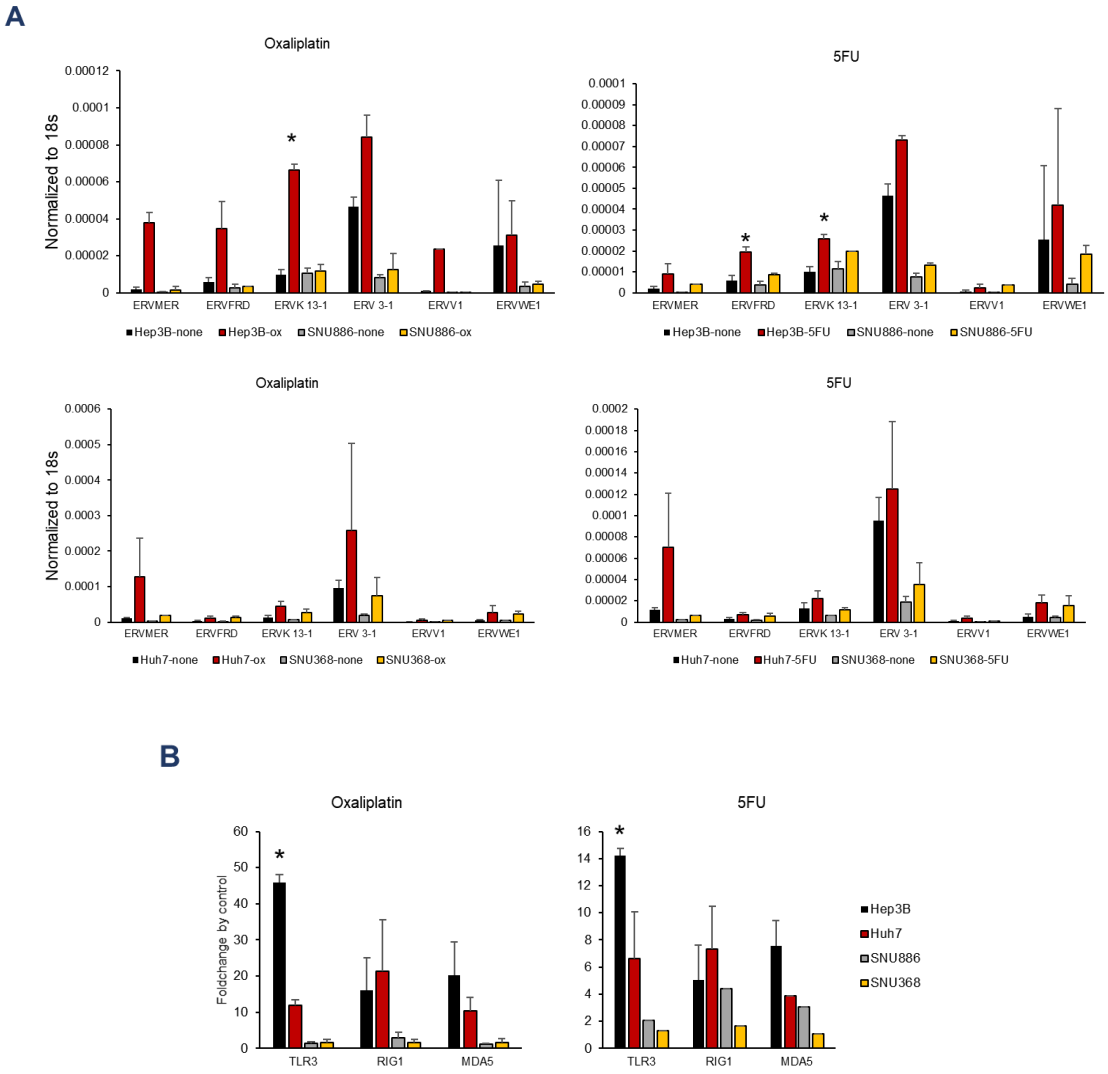

Figure 2. Importance of dsRNAs from ERVs for ISGs induction after chemotherapy

(A-B) Hep3B, Huh7, SNU886 and SNU368 cells were treated or not with 5 µM oxaliplatin or 10 µM 5-FU for 5 days, and expression of (A) ERVs transcripts and (B) PRRs was analyzed by qRT-PCR. Relative levels of expression were normalized to 18S ribosomal RNA. Data are shown as mean ± SD (n=5).

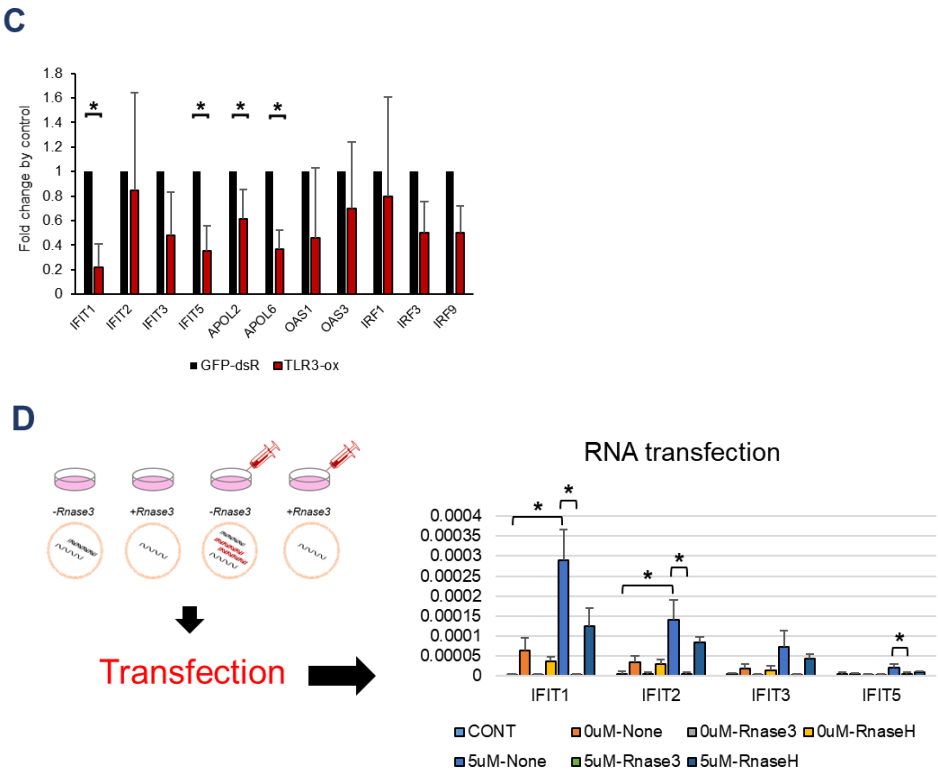

Figure 2.

(C) Hep3B cells were transduced with control (GFP) or TLR3-targeting lentiCRISPR vectors and selected for 7 days with 1 μg/ml puromycin. ISGs expression was analyzed by qRT-PCR after 5 μM oxaliplatin for 3 days or not. Relative levels of expression were normalized to 18S ribosomal RNA and untreated cells. Data are shown as mean ± SD (n=5).

(D) Left, Schematic representation of RNase-treated RNA transfection experiment. Hep3B cells were treated with 5 μM oxaliplatin or vehicle for 72 h and then total RNA was extracted. Five micrograms of total RNAs were treated with 2 U/μg RNase III, 10 U/μg RNase H or not for 30 min at 37 °C. Subsequently, 2 μg of RNA was transfected into Hep3B recipient. Right, qRT-PCR analysis of IFITs mRNA in Hep3B cells transfected with the same amount of RNA as indicated. Data are mean ± SD (n=3).

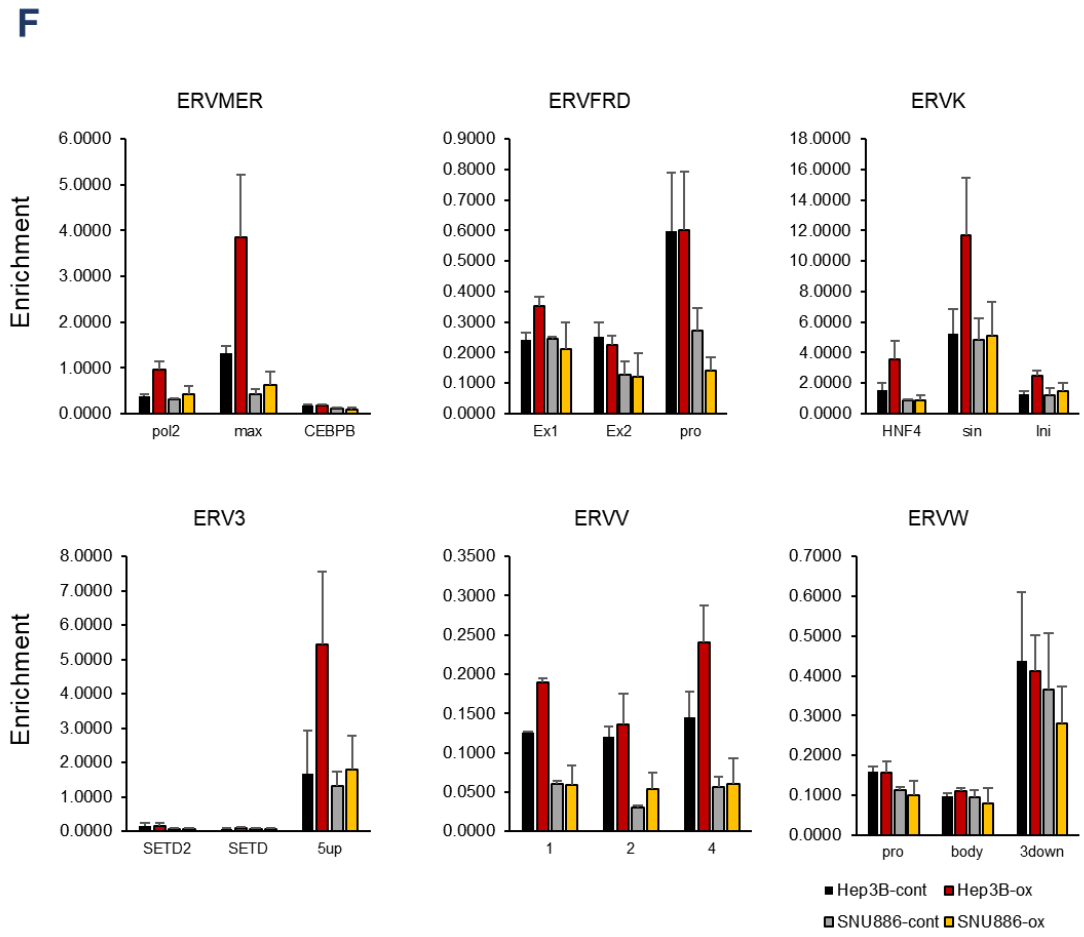

Figure 2.

(E) Hep3B and SNU886 were treated or not with 5 μM oxaliplatin for 3 days. ChIP assay was performed using antibodies against AcH3 and IgG as control. Mean ± SEM, n = 3 biological replicates.

STAT1/2 binding on the promoter region is crucial for the transcriptional induction of ISGs by chemotherapy

Above results demonstrate that upon the recognition of ERV-derived dsRNA after oxaliplatin or 5-FU, transcription of diverse ISGs is simultaneously activated to evoke anti-tumor effect of viral mimicry that may be crucial for the chemo-therapeutic success in HCC cells. Therefore, it is of great interest to understand the molecular mechanisms underlying the coordinate transcriptional regulation of ISGs after chemotherapy. In order to dissect the possible mechanisms more effectively, I used the synthetic analog of viral dsRNA, poly (I:C) [30], to model viral mimicry induced by dsRNAs generated from ERVs after chemotherapy [25, 28]. First, I found that ISGs tested for transcriptional activation after chemotherapy was significantly upregulated by poly (I:C) treatment for 6 h in Hep3B cells (Figure 3A). However, the induction of ISGs after poly (I:C) was abrogated by disruption of TLR3 (data not shown), demonstrating that poly (I:C) activates the same signaling pathway with ERV-derived dsRNA after chemoagnets treatment in Hep3B cells. Similar to oxaliplatin or 5-FU treatment (Figure 1A), the exogenous addition of poly (I:C) significantly enhanced the phosphorylation of STAT1 in Hep3B cells (Figure 3B).

Next, I examined if STAT1/2 are the transcription factor that transduce ISGs expression and acts as transcriptional regulators after chemotherapy. As STAT1/2 is known to directly binds to gene promoter region to regulate ISGs expression [11], I performed chromatin immunoprecipitation (ChIP) assay to confirm the enrichment of STAT1/2 within the target gene locus. Among the variable genes, interferon-induced

protein with tetratricopeptide repeats (IFIT) gene family (IFIT1, IFIT2, IFIT3 and IFIT5) showed more that 20-fold simultaneous induction after the poly (I:C) treatment in Hep3B cells (Figure 3A). With the increased expression of the IFIT genes (Figure 3A), the binding of STAT1/2 within the IFIT locus was enhanced by poly (I:C) treatment (Figure 3C). The enrichment of RNA polymerase II (Pol II) and AcH3 which are the active marker for RNA expression [29] also increased after poly (I:C) treatment (Figure 3C). I similarly observed the increased STAT1/2 binds within the promoter region of IFIT locus after oxaliplatin or 5-FU treatment in Hep3B cells (Figure 3D and 3E). I obtained similar results with other ISGs (data not shown). Considering the fact that depletion of STAT1/2 can lead to reduction of chemotherapy-mediated ISGs expression (Figure 1E), STAT1/2 binding within the IFIT locus might be correlate with the transcriptional induction of the target genes after oxaliplatin or 5-FU treatment.

STAT1/2 mediated higher-order chromatin structure is crucial for the transcriptional regulation of IFIT locus after chemotherapy

Increasing evidence has indicated that higher-order chromatin organization is functionally important for transcriptional regulation of genes during development and differentiation [19, 31, 32]. Very interestingly, recently it has been shown that interferon-induced transmembrane protein (IFITM) locus forms long-range chromatin interactions, which may provide the adequate controls to coordinately alter IFITM1, IFITM2 and IFITM3 gene expression in response to the virus infection [33]. Since the STAT1/2-binding motifs were preferentially localized at the transcription start site of all type I IFN gene signatures [34], I speculated that the binding of STAT1/2 on the IFIT locus may form the higher-order chromatin structure and regulate the expression of these genes. To identify this hypothesis, I carried out a chromosome conformation capture (3C) analysis [35] to assess the proximity of chromatin across the IFIT locus in Hep3B cells. As expected STAT1/2 binding sites within the transcriptional start site of the IFIT1 gene strongly interacted with the other STAT1/2 binding sites of IFIT locus in Hep3B cells after poly (I:C) treatment (Figure 3F). Our results in chemoagent-treated Hep3B cells were similar to the previous results obtained from poly (I:C)-treated Hep3B cells (data not shown), suggesting that the transcriptional upregulation of IFIT locus were associated with tighter chromatin structure, bringing each target genes into physical proximity after chemotherapy.

To identify whether STAT1/2 binding is essential for long-range chromatin interactions of IFIT locus, I repeated 3C assay in STAT1/2-depleted Hep3B cells.

Interestingly, I found that higher-order chromatin organization of IFIT locus was significantly abolished by STAT1 deficiency (Figure 3G), insisting that STAT1/2 may form long-range chromatin interactions at the IFIT locus to facilitate transcription and a high level expression of IFIT genes in Hep3B cells after chemotherapy.

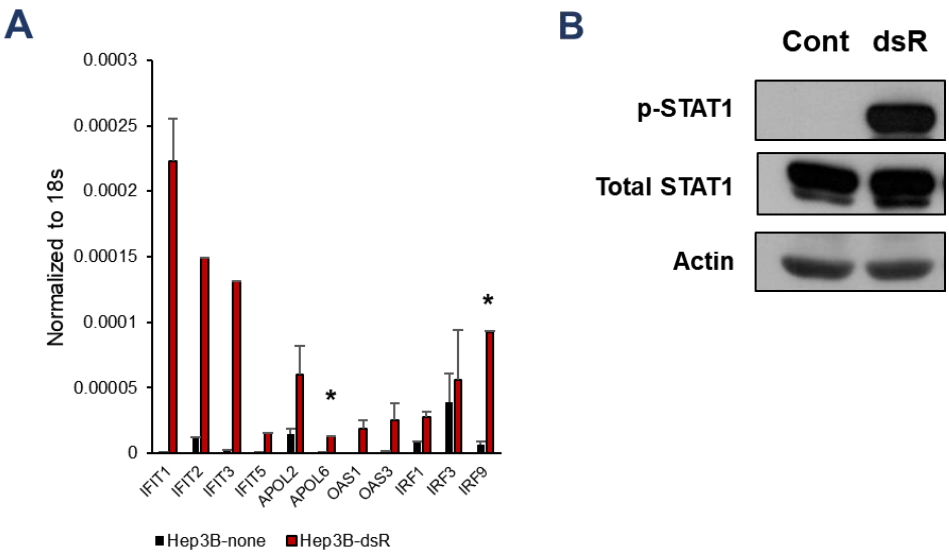

Figure 3. STAT1/2-mediated higher-order chromatin structure is crucial for the transcriptional regulation of IFIT locus

(A-D) Hep3B cells were treated or not with 20 μg/ml poly (I:C) for 6 h. (A) ISGs expression was analyzed by qRT-PCR. Relative levels of expression were normalized to 18S ribosomal RNA. Data are shown as mean ± SD (n=5). (B) Total cell extracts were prepared for western blot analysis with indicated antibodies. Actin was used as loading control.

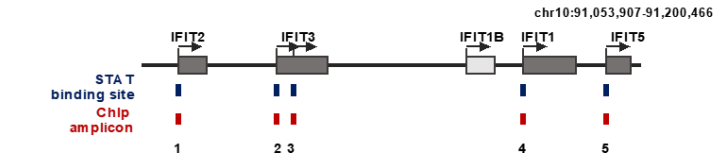
chr10:91,053,907-91,200,466
IFIT2
IFIT3
IFIT1B
IFIT1
IFIT5
STAT binding site
ChIp amplicon
1
2 3
4
5

C

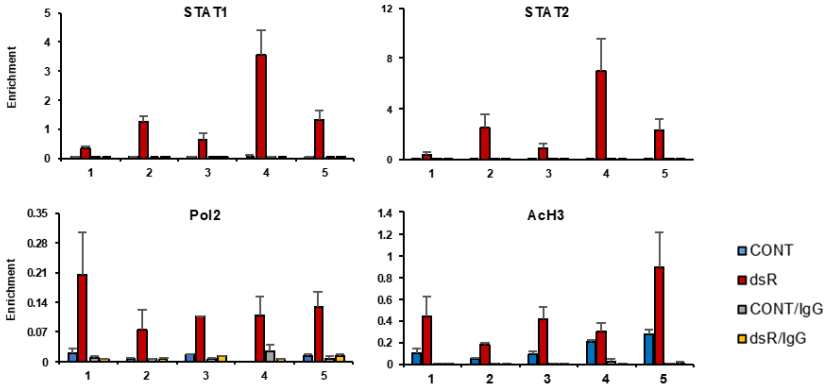
STAT1
STAT2
Pol2
AcH3
Enrichment
CONT
dsR
CONT/IgG
dsR/IgG

D

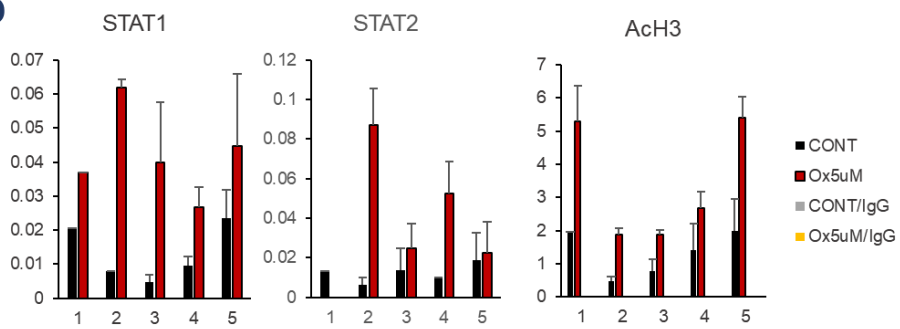
STAT1
STAT2
AcH3
CONT
Ox5uM
CONT/IgG
Ox5uM/IgG

E

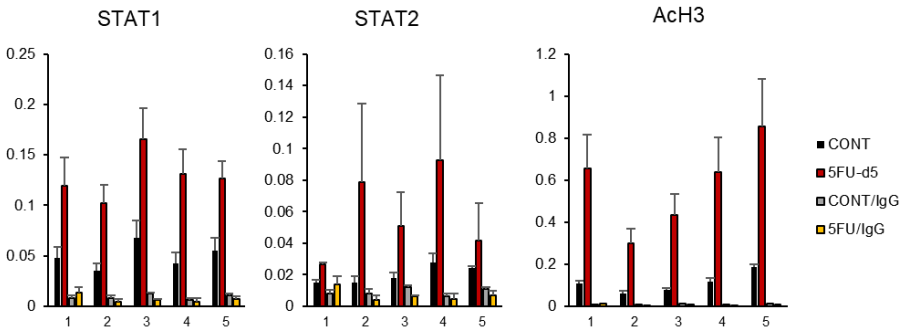
STAT1
STAT2
AcH3
CONT
5FU-d5
CONT/IgG
5FU/IgG

Figure 3.

(C) IFIT locus on chromosomes 10 is illustrated to scale. STAT1/2 binding sites are indicated by blue box, and the primer pairs used for ChIP assays are shown as red box with labels below. The black arrow represents the transcriptional start site. The ChIP assay was performed using antibodies against STAT1, STAT2, Pol II, AcH3, and IgG as control. Mean ± SEM, n = 3 biological replicates.

(D-E) Hep3B cells were treated or not with (A) 5 μM oxaliplatin or (B) 10 μM 5-FU for 3 days and then, ChIP assay was performed with STAT1, STAT2, and AcH3 antibodies. IgG served as control. Mean ± SEM, n = 3 biological replicates.

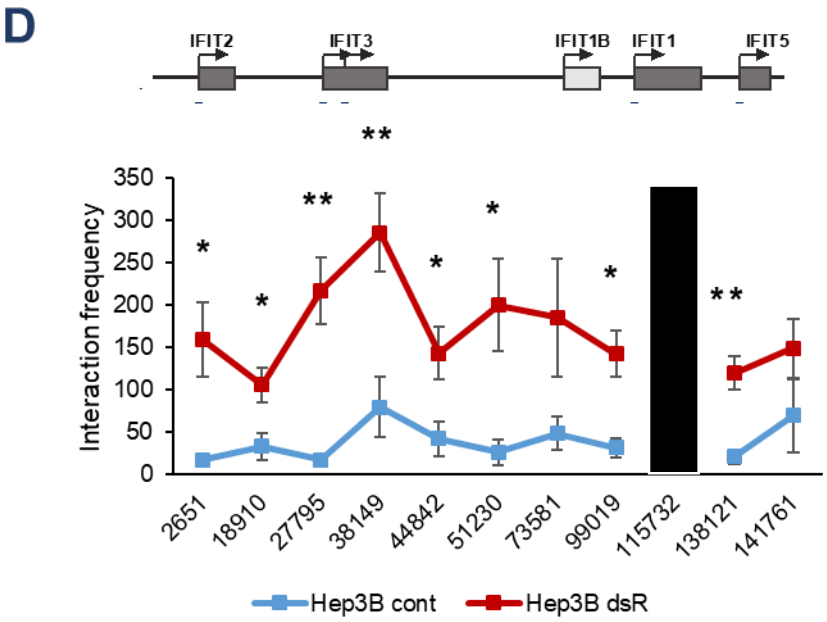

Figure 3.

(F) Relative crosslinking frequencies among STAT1/2-binding sites in the IFIT locus were measured with a 3C assay after treatment with vehicles (blue line) or poly I:C (red line). Black shading indicates the anchor fragment at the STAT1/2 binding site of IFIT1. The maximum crosslinking frequency was set to 1 (mean ± SEM, n =5)

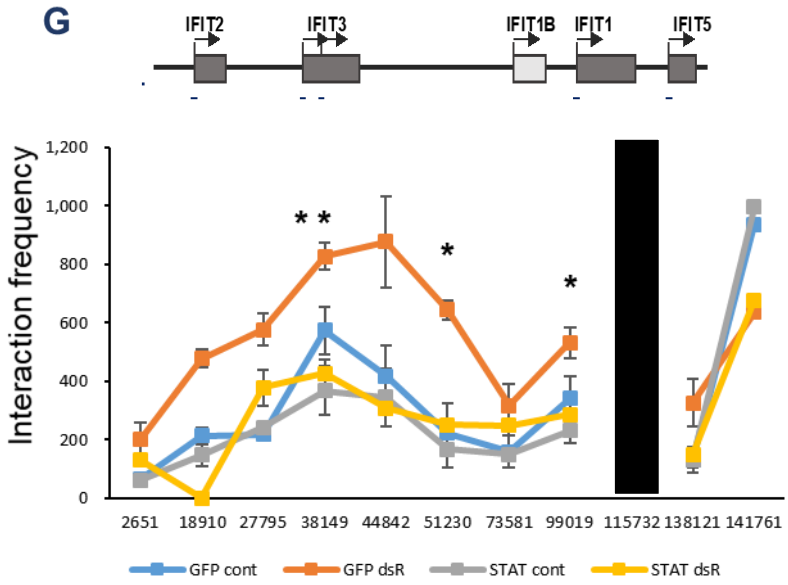

Figure 3.

(G) Hep3B cells were transduced with control (GFP) or STAT1/2-targeting lentiCRISPR vectors and selected in 1 μg/ml puromycin. After 7 days, transduced cells were plated into 96-well plates, and further expanded approximately 30 days to make single clone. Relative crosslinking frequencies among STAT1/2-binding sites in the IFIT locus were measured with a 3C assay in GFP and KO clone after treatment of 20 μg/ml poly (I:C) for 6 hours or not. Black shading indicates the anchor fragment at the STAT1/2 binding site of IFIT1. The maximum crosslinking frequency was set to 1 (mean ± SEM, n =3)

Higher-order chromatin structure is crucial for the coordinated transcriptional regulation of ISGs by chemotherapy

To further test if STAT1/2 binding is a prerequisite for the coordinated transcriptional regulation of ISGs after chemotherapy, I tried to delete the STAT1/2 binding site within IFIT1 gene using CRISPR/Cas9 system (Figure 4A) [31]. Very interestingly, I found that deletion of the STAT1/2 binding site within the promoter region of IFIT1 gene completely reduced the expression of entire set of IFIT family after dsRNA or chemoagent treatment (Figure 4B-C). Consistent with decreased expression of IFIT family, enrichment of STAT1/2 on the other STAT1/2 binding sites within IFIT locus were also significantly reduced when STAT1/2 binding site was deleted (Figure 4D). In addition, the physical proximity between STAT1/2 binding sites within these locuses were abolished by disruption of the STAT1/2 binding (Figure 4E). Furthermore, inhibition of STAT1/2 binding within IFIT1 gene resulted in a striking reduction in the transcriptional activation of other ISGs after dsRNA or chemo-treatment (Figure 4B-C), suggesting that enrichment of STAT1/2 within IFIT1 gene not only affects the expression of IFIT locus genes, but also have a global influence on the transcription of ISGs after chemotherapy.

The spatial proximities among STAT1/2 binding sites between IFIT and OAS locus were decreased by inhibition of the STAT1/2 binding within IFIT1 gene in agreement with the reduction of STAT1/2 enrichment on these region (Figure 4F). However, no significant changes on the basal expression or phosphorylation level of STAT1, reflecting its activation, were detected when STAT1/2 binding within IFIT1 gene was eliminated by CRISPR/Cas9 technology (Figure 4G).

Collectively, these results suggest the possibility that the enrichment of STAT1/2 affects coordinate gene transcription by facilitating long-range interactions between members of many ISGs families after chemotherapy (Figure 5).

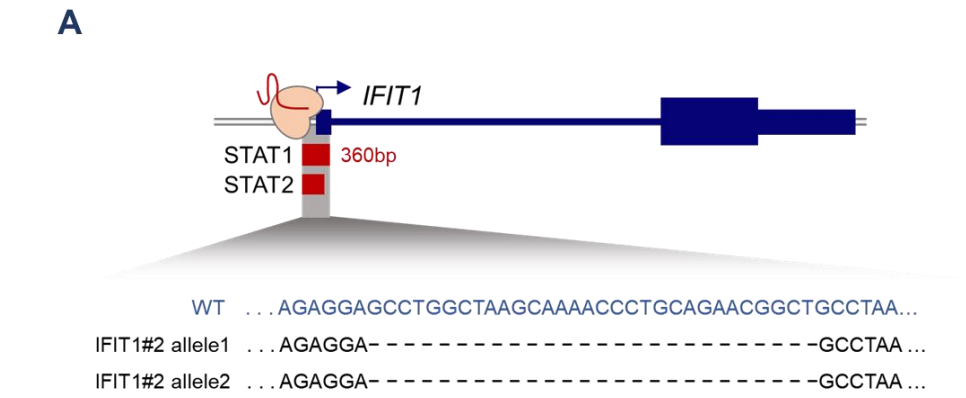
A
IFIT1
STAT1
STAT2
360bp
WT . . . AGAGGAGCCTGGCTAAGCAAAACCCTGCAGAACGGCTGCCTAA...
IFIT1#2 allele1 . . . AGAGGA- -GCCTAA ...
IFIT1#2 allele2 . . . AGAGGA- -GCCTAA ...

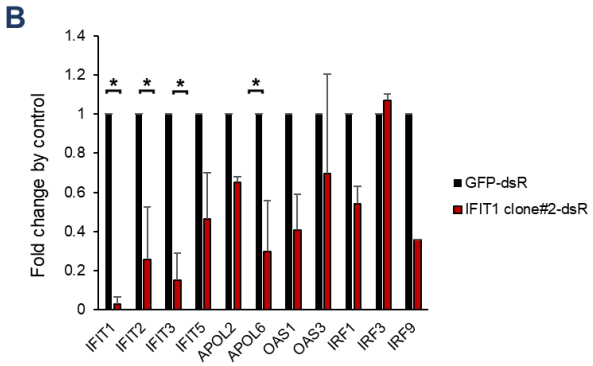
B
Fold change by control
1.4
1.2
1
0.8
0.6
0.4
0.2
0
IFIT1
IFIT2
IFIT3
IFIT5
APOL2
APOL6
OAS1
OAS3
IRF1
IRF3
IRF9
GFP-dsR
IFIT1 clone#2-dsR

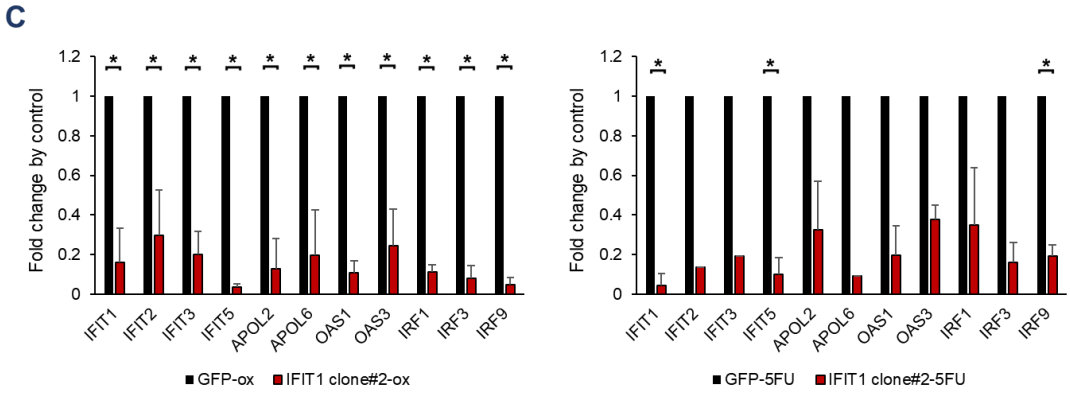
C
Fold change by control
1.2
1
0.8
0.6
0.4
0.2
0
IFIT1
IFIT2
IFIT3
IFIT5
APOL2
APOL6
OAS1
OAS3
IRF1
IRF3
IRF9
GFP-ox
IFIT1 clone#2-ox
GFP-5FU
IFIT1 clone#2-5FU

Figure 4. STAT1/2 binding is a prerequisite for the coordinated transcriptional regulation of ISGs

(A) Stable single clone (IFIT1-clone#1) harboring deleted STAT1/2 binding region on the both alleles in the IFIT1 promoter was screened and confirmed by DNA sequencing analysis.

(B-C) qRT-PCR analysis of ISGs expression in GFP and IFIT1-clone#1 cells after treatment of (B) 20 μg/ml poly (I:C) for 6 h or (C) 5 μM oxaliplatin and 10 μM 5-FU for 3 days. Relative levels of expression were normalized to 18S ribosomal RNA and untreated cells. Data are shown as mean ± SD (n=3).

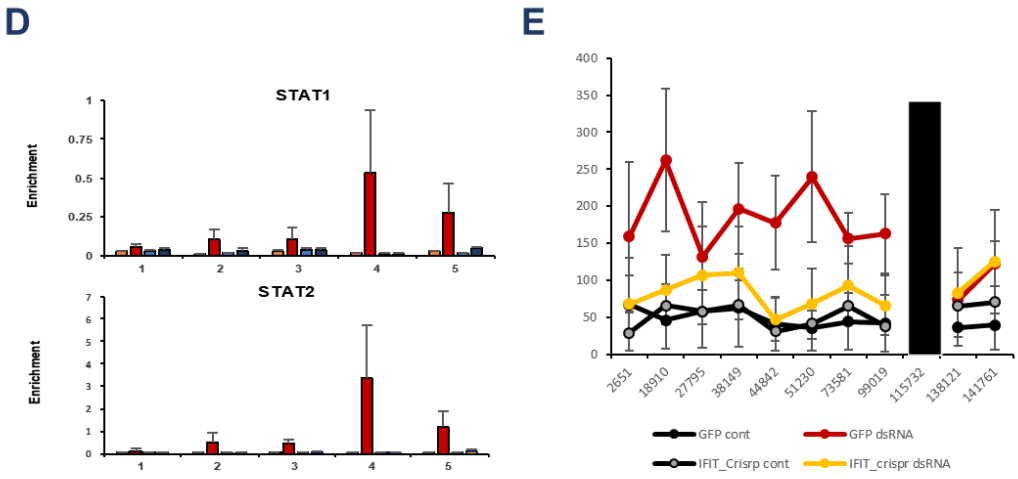
D
STAT1
Enrichment
STAT2
Enrichment
E
GFP cont
GFP dsRNA
IFIT_Crisrp cont
IFIT_crispr dsRNA

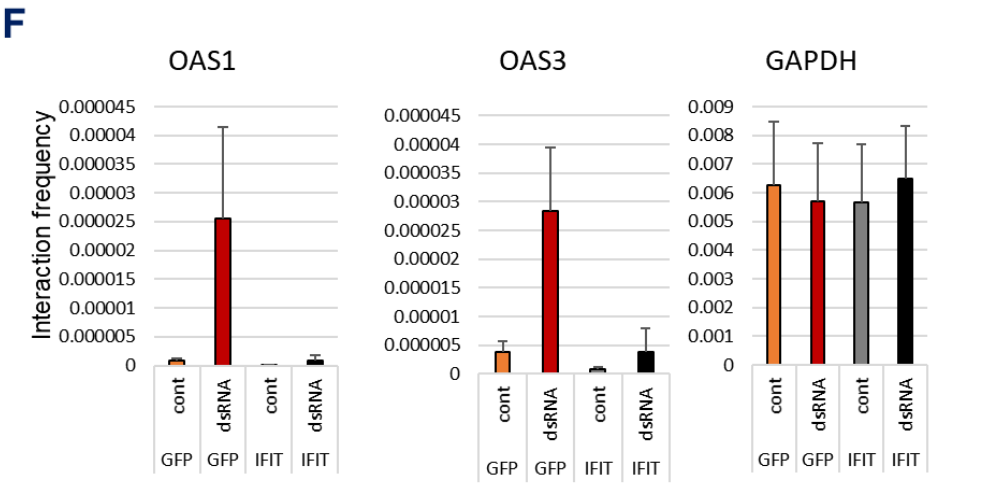
F
OAS1
OAS3
GAPDH
Interaction frequency
cont
dsRNA
GFP
IFIT

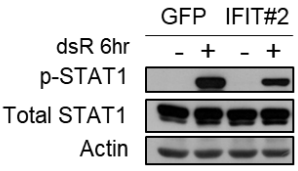
G
GFP
IFIT#2
dsR 6hr
p-STAT1
Total STAT1
Actin

Figure 4.

(D-E) Stable GFP or IFIT1-clone#1 was treated or not with 20 μg/ml poly (I:C) for 6 h. (D) ChIP assay was performed in using antibodies against STAT1 and STAT2. Mean ± SEM, n = 3 biological replicates. (E-F) Relative crosslinking frequencies among STAT1/2-binding sites in (E) the IFIT locus and (F) the OAS locus were measured with a 3C assay in GFP and KO clone after treatment of poly (I:C) or not. The maximum crosslinking frequency was set to 1 (mean ± SEM, n =3)

(G) Stable GFP and two single clones (IFIT1-clone#1 and IFIT1-clone#2) having deleted STAT1/2 binding region were treated or not with 20 μg/ml poly (I:C) for 6 h.

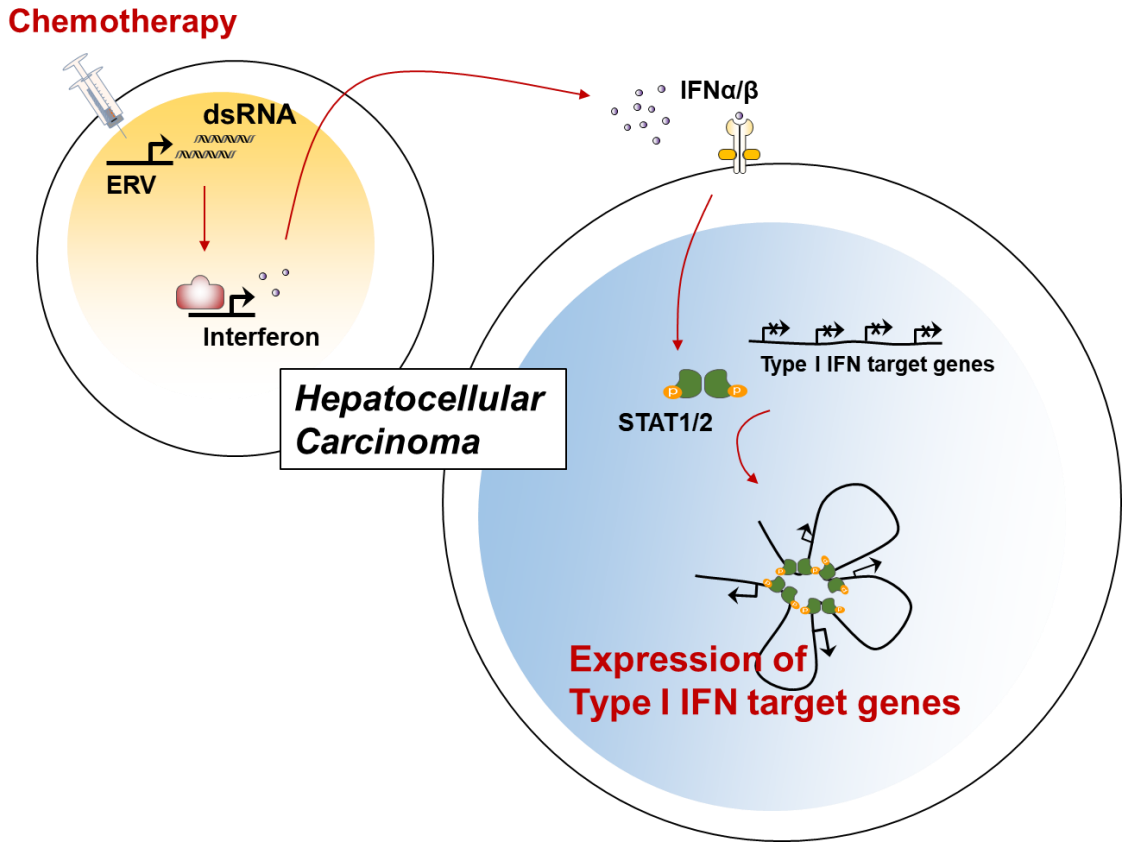

Figure 5. Proposed model for STAT1/2-mediated higher-order chromatin structure after chemotherapy in HCC cells

Discussion

Our understanding of natural immune responses to cancer has further improved following the realization the dual opposing role of immunity- host protection and tumor progression [32, 33]. This cancer immunoediting hypothesis emphasizes that extrinsic immune system either can block tumor growth or can facilitate tumor outgrowth by sculpting tumor immunogenicity [33, 34]. To win the fight against cancer, it is crucial to stimulate the host immune response and restrict the capacity of developing tumor to escape immune control [4, 32]. Although conventional anti-cancer chemotherapy is generally thought to act through selective killing of tumor cells or by irreversibly arresting their growth [5], accumulating evidence indicates that the immune system make a crucial contribution to the success of this anti-cancer chemotherapy [2]. It is now known that some of the cytotoxic drugs elicit specific cellular responses that render tumor cell death immunogenic [6, 35, 36]. These immunogenic cell death evokes immune responses as it is associated with the emission of danger signals that activate the immune response [1]. Therefore, understanding how chemotherapy stimulate exposure of specific DAMPs and their association with immunogenic cell death will facilitate the development of therapeutic regimens that can activate anti-tumor immunosurveillance [2, 3].

Similarly, treatment of low-dose of demethylating agent, 5-aza-CdR, upregulate immune response in tumor cells through the viral defense pathway [25, 28]. Thus, this phenomenon is called as viral mimicry, as activated type I IFN related gene signatures are similar to those induced by viral pathogens [6, 28]. Interestingly, they found that treatment of 5-aza-CdR induce transcription of viral defense genes through cancer cell-

autonomous release of dsRNAs derived from endogenous ERVs which can mimic viral infection during cancer treatment [25, 28]. These results inspired us to speculate that chemotherapy also can induce viral defense genes via dsRNAs derived from ERVs in HCC, one of the most common cancer, which is thought to result from persistent, nonspecific activation of the immune system within the chronically inflamed liver, causing repeated cycles of tissue damage, repair, and eventually tumorigenesis [37, 38]. In this study, we found that treatment of chemotherapeutic agents, such as oxaliplatin or 5-FU, activate ISGs transcription with concomitant induction of ERVs in HCC cells (Fig. 2A). Considering the fact that the treatment of RNase III which specifically degrade dsRNA, completely abolished the ISGs expression after chemotherapy, chemotherapeutic agents-mediated ISGs induction might be caused by dsRNAs derived from ERVs but not single-stranded RNA nor double-stranded DNA (Fig. 2E). In addition, I also identified that PRR such as TLR3 and/or RIG1, endosomal receptor for dsRNAs [30], worked as an adaptor to transmit activation signal induced by dsRNAs into type I IFN-STAT1 signaling pathway (Fig. 2C and D). While DNA methylation-mediated transcriptional silencing of ERVs are frequently detected in several types of cells [25, 28, 39], HCC cells were devoid of DNA methylation near ERVs (data not shown), suggesting the individual methylation status of ERVs are not correlated with ERVs induction after chemotherapy in HCC cells. Instead, the dynamics of AcH3 modifications might confer up-regulation of ERVs during chemo treatment in HCC cells. However, histone H3 K9 tri-methylation (H3K9me3) which is known as repressive marker for ERV elements [40] was not changed after chemotherapy (data not shown).

Upon receiving external signals, distinct signaling pathways are activated to

culminate in the induction or repression of defined sets of genes [41]. The fine tuning of numerous functionally related genes in spatiotemporal manner demands delicate manipulation [41]. Interestingly, functionally related and co-regulated genes often form multi-gene loci in mammalian genomes [42]. For example, genes involved in execution of keratinocyte-specific gene expression programs are clustered in at least three evolutionally conserved regions, including the epidermal differentiation complex and Keratin type I and type II loci [43]. So given the growing appreciation of chromatin structure as an important element regulating gene expression [13, 16, 18], We speculate that higher-order chromatin folding via STAT1/2 may facilitate functional interactions between type I IFN related genes after chemotherapy in HCC cells. In this study, We found that the enrichment of STAT1/2 on the IFIT locus is necessary for the simultaneous transcription of IFIT gene family and for higher-order structure of IFIT locus, demonstrating that gene transcription and chromatin organization are closely linked with coordinate regulation of IFIT locus after treatment of chemotherapeutic agents in HCC cells (Fig. 5). Furthermore, We subsequently identified the spatial proximity between the IFIT1 gene and other ISGs were completely reduced after perturbation of the STAT1/2 binding on the promoter region of IFIT1 gene (Fig. 4), suggesting that STAT1/2 binding on one site may stabilize the interaction with other multiple STAT1/2 enrichment sites throughout the genome after chemotherapy. This finding is consistent with the recent results that long-range chromatin interaction is responsible for coordinated regulation of IFITM locus, one of the best known viral defense genes [44]. Therefore, our results further supports the idea that proper higher-order chromatin folding in the three-dimensional nuclear space is important in establishing functional interactions between

the promoters involved in controlling signal-specific gene transcription for numerous genes [42].

Taken together, we have demonstrated that transcription of diverse ISGs is simultaneously activated by forming higher-order chromatin structures to evoke anti-tumor effect that may be crucial for the chemo-therapeutic success.

References

1. Apetoh, L., et al., *Immunogenic chemotherapy: discovery of a critical protein through proteomic analyses of tumor cells.* Cancer Genomics Proteomics, 2007. **4**(2): p. 65-70.
2. Holzel, M., A. Bovier, and T. Tuting, *Plasticity of tumour and immune cells: a source of heterogeneity and a cause for therapy resistance?* Nat Rev Cancer, 2013. **13**(5): p. 365-76.
3. Medler, T.R., T. Cotechini, and L.M. Coussens, *Immune response to cancer therapy: mounting an effective antitumor response and mechanisms of resistance.* Trends Cancer, 2015. **1**(1): p. 66-75.
4. Vinay, D.S., et al., *Immune evasion in cancer: Mechanistic basis and therapeutic strategies.* Semin Cancer Biol, 2015. **35 Suppl**: p. S185-S198.
5. Cheung-Ong, K., G. Giaever, and C. Nislow, *DNA-damaging agents in cancer chemotherapy: serendipity and chemical biology.* Chem Biol, 2013. **20**(5): p. 648-59.
6. Sistigu, A., et al., *Cancer cell-autonomous contribution of type I interferon signaling to the efficacy of chemotherapy.* Nat Med, 2014. **20**(11): p. 1301-9.
7. Ma, Y., et al., *Contribution of IL-17-producing gamma delta T cells to the efficacy of anticancer chemotherapy.* J Exp Med, 2011. **208**(3): p. 491-503.
8. Apetoh, L., et al., *The interaction between HMGB1 and TLR4 dictates the outcome of anticancer chemotherapy and radiotherapy.* Immunol Rev, 2007. **220**: p. 47-59.
9. Garg, A.D., et al., *Molecular and Translational Classifications of DAMPs in Immunogenic Cell Death.* Front Immunol, 2015. **6**: p. 588.
10. Bowie, A.G. and L. Unterholzner, *Viral evasion and subversion of pattern-recognition receptor signalling.* Nat Rev Immunol, 2008. **8**(12): p. 911-22.
11. Ivashkiv, L.B. and L.T. Donlin, *Regulation of type I interferon responses.* Nat Rev Immunol, 2014. **14**(1): p. 36-49.
12. de Wit, E., et al., *The pluripotent genome in three dimensions is shaped around pluripotency factors.* Nature, 2013. **501**(7466): p. 227-31.

13. Nagano, T., et al., *Single-cell Hi-C reveals cell-to-cell variability in chromosome structure.* Nature, 2013.
14. Schoenfelder, S., et al., *Preferential associations between co-regulated genes reveal a transcriptional interactome in erythroid cells.* Nat Genet, 2010. **42**(1): p. 53-61.
15. de Wit, E., et al., *CTCF Binding Polarity Determines Chromatin Looping.* Mol Cell, 2015. **60**(4): p. 676-84.
16. Phillips-Cremins, J.E., et al., *Architectural protein subclasses shape 3D organization of genomes during lineage commitment.* Cell, 2013. **153**(6): p. 1281-95.
17. Dixon, J.R., et al., *Topological domains in mammalian genomes identified by analysis of chromatin interactions.* Nature, 2012. **485**(7398): p. 376-80.
18. Wang, X.Q.D. and J. Dostie, *Chromosome folding and its regulation in health and disease.* Curr Opin Genet Dev, 2017. **43**: p. 23-30.
19. Ji, X., et al., *3D Chromosome Regulatory Landscape of Human Pluripotent Cells.* Cell Stem Cell, 2016. **18**(2): p. 262-75.
20. Yun, J., et al., *Reduced cohesin destabilizes high-level gene amplification by disrupting pre-replication complex bindings in human cancers with chromosomal instability.* Nucleic Acids Res, 2016. **44**(2): p. 558-72.
21. Song, S.H., et al., *Aberrant GATA2 epigenetic dysregulation induces a GATA2/GATA6 switch in human gastric cancer.* Oncogene, 2018. **37**(8): p. 993-1004.
22. Park, Y.L., et al., *Activation of WNT/beta-catenin signaling results in resistance to a dual PI3K/mTOR inhibitor in colorectal cancer cells harboring PIK3CA mutations.* Int J Cancer, 2019. **144**(2): p. 389-401.
23. Shalem, O., et al., *Genome-scale CRISPR-Cas9 knockout screening in human cells.* Science, 2014. **343**(6166): p. 84-7.
24. Dhir, A., et al., *Mitochondrial double-stranded RNA triggers antiviral signalling in humans.* Nature, 2018. **560**(7717): p. 238-242.
25. Chiappinelli, K.B., et al., *Inhibiting DNA Methylation Causes an Interferon Response in Cancer via dsRNA Including Endogenous Retroviruses.* Cell, 2015.

162(5): p. 974-86.

26. Sanjana, N.E., O. Shalem, and F. Zhang, *Improved vectors and genome-wide libraries for CRISPR screening.* Nat Methods, 2014. **11**(8): p. 783-784.
27. Trinchieri, G., *Type I interferon: friend or foe?* J Exp Med, 2010. **207**(10): p. 2053-63.
28. Roulois, D., et al., *DNA-Demethylating Agents Target Colorectal Cancer Cells by Inducing Viral Mimicry by Endogenous Transcripts.* Cell, 2015. **162**(5): p. 961-73.
29. Rodriguez-Paredes, M. and M. Esteller, *Cancer epigenetics reaches mainstream oncology.* Nat Med, 2011. **17**(3): p. 330-9.
30. Matsumoto, M. and T. Seya, *TLR3: interferon induction by double-stranded RNA including poly(I:C).* Adv Drug Deliv Rev, 2008. **60**(7): p. 805-12.
31. Kang, J., Y.W. Kim, and A. Kim, *Histone variants H3.3 and H2A.Z are incorporated into the beta-globin locus during transcription activation via different mechanisms.* Biochim Biophys Acta Gene Regul Mech, 2018.
32. Schreiber, R.D., L.J. Old, and M.J. Smyth, *Cancer immunoediting: integrating immunity's roles in cancer suppression and promotion.* Science, 2011. **331**(6024): p. 1565-70.
33. Dunn, G.P., L.J. Old, and R.D. Schreiber, *The immunobiology of cancer immunosurveillance and immunoediting.* Immunity, 2004. **21**(2): p. 137-48.
34. Mittal, D., et al., *New insights into cancer immunoediting and its three component phases--elimination, equilibrium and escape.* Curr Opin Immunol, 2014. **27**: p. 16-25.
35. Bracci, L., et al., *Immune-based mechanisms of cytotoxic chemotherapy: implications for the design of novel and rationale-based combined treatments against cancer.* Cell Death Differ, 2014. **21**(1): p. 15-25.
36. Emens, L.A. and G. Middleton, *The interplay of immunotherapy and chemotherapy: harnessing potential synergies.* Cancer Immunol Res, 2015. **3**(5): p. 436-43.
37. Coussens, L.M. and Z. Werb, *Inflammation and cancer.* Nature, 2002. **420**(6917): p. 860-7.

38. Grivennikov, S.I., F.R. Greten, and M. Karin, *Immunity, inflammation, and cancer.* Cell, 2010. **140**(6): p. 883-99.
39. Grow, E.J., et al., *Intrinsic retroviral reactivation in human preimplantation embryos and pluripotent cells.* Nature, 2015. **522**(7555): p. 221-5.
40. Maksakova, I.A., et al., *H3K9me3-binding proteins are dispensable for SETDB1/H3K9me3-dependent retroviral silencing.* Epigenetics Chromatin, 2011. **4**(1): p. 12.
41. Cheung, P., C.D. Allis, and P. Sassone-Corsi, *Signaling to chromatin through histone modifications.* Cell, 2000. **103**(2): p. 263-71.
42. Fessing, M.Y., *Gene regulation at a distance: higher-order chromatin folding and the coordinated control of gene transcription at the epidermal differentiation complex locus.* J Invest Dermatol, 2014. **134**(9): p. 2307-2310.
43. Oh, I.Y., et al., *Regulation of the dynamic chromatin architecture of the epidermal differentiation complex is mediated by a c-Jun/AP-1-modulated enhancer.* J Invest Dermatol, 2014. **134**(9): p. 2371-2380.
44. Li, P., et al., *Coordinated regulation of IFITM1, 2 and 3 genes by an IFN-responsive enhancer through long-range chromatin interactions.* Biochim Biophys Acta Gene Regul Mech, 2017. **1860**(8): p. 885-893.

국문 초록

Type I interferon signaling pathway 는 세포독성항암제에 의해 활성화되는 것으로 알려져 있으며, 이의 효과로 anti-tumor immune response 현상을 야기한다. Type I interferon signaling pathway 는 바이러스와 같은 병원체 감염에 의해 활성화 되는 신호전달체계이다. 바이러스의 감염이 존재하지 않으나 마치 감염이 있는 것처럼 반응하여 이러한 신호체계를 활성화시키는 현상을 viral mimicry 라 일컫는다. 본 논문에서는 세포독성항암제 처리로 인하여 간암세포 내에 내재되어 있던 Endogenous retrovirus 의 발현이 활성화 되어 그의 전사체인 dsRNA 가 생성되는 viral mimicry 현상을 확인하였다. 이 때, dsRNA 가 주요 매개체가 되어 다양한 Interferon stimulated genes (ISGs)의 발현을 동시다발적으로 증가시키게 되는데, 이 과정에서 signal transducer and activator of transcription 1/2 라고 알려진 STAT1 과 STAT2 에 의한 크로마틴 삼차구조 형성이 중요한 역할을 한다는 것을 밝혔다. 크로마틴 삼차구조의 형성은 유전자의 발현을 조절하는 것으로 알려져 있는데, 염색체 상에서 멀리 떨어져 있는 유전자들로 하여금 물리적으로 가깝게 하여 효과적인 유전자발현을 조절하게 된다.

세포독성항암제 혹은 dsRNA 합성물질을 처리하게 되면, ISG locus 에서의 STAT1 과 2 의 결합이 증가함과 동시에 삼차구조가 형성되는 것을 확인하였다. 이러한 현상은 STAT1/2 를 CRISPR/Cas9 KO system 을 이용하여 발현을 감소시켰을 때 사라지는 것을 증명하였다. 또한, IFIT1 에서 STAT1/2 의 결합하는 부위를 CRISPR system 을 이용하여 잘라냈을 때에도 동일한 현상이 나타남을 증명하였다. 세포독성항암제에 대한 감수성은 STAT1 의 발현이 저해되었을 때 감소하는 양상을 보였다.

이를 바탕으로 STAT1/2 를 매개로 한 크로마틴 삼차구조가 ISG 의 발현을 결정하는 데에 중요한 역할을 하며, 이는 세포독성항암제에 대한 효과에 영향을 미치는 것을 본 논문을 통해 규명하였다.

주 요 어 : 암, 후성유전학, Higher-order chromatin structure, Type I interferon signaling, viral mimicry

학 번 : 2017-22991